CELL WALL DOMAIN AND MOISTURE CONTENT INFLUENCE SOUTHERN PINE ELECTRICAL CONDUCTIVITY[1]

*Samuel L. Zelinka**†*

Project Leader
Building and Fire Sciences
E-mail: szelinka@fs.fed.us

Leandro Passarini†

Postdoctoral Researcher
Building and Fire Sciences
USDA Forest Service, Forest Products Laboratory
Madison, WI
E-mail: lpassarini@fs.fed.us

José L. Colon Quintana

Student
University of Puerto Rico Mayagüez
Mayagüez, Puerto Rico
E-mail: jose.colon@68@upr.edu

Samuel V. Glass†

Research Physical Scientist
Building and Fire Sciences
E-mail: svglass@fs.fed.us

Joseph E. Jakes†

Research Materials Engineer
Forest Biopolymers Science and Engineering
E-mail: jjakes@fs.fed.us

Alex C. Wiedenhoeft

Research Botanist
Center for Wood Anatomy Research
USDA Forest Service, Forest Products Laboratory
Madison, WI
E-mail: awiedenhoeft@fs.fed.us

(Received August 2015)

Abstract. Recent work has highlighted the importance of movement of chemicals and ions through the wood cell wall. This movement depends strongly on MC and is necessary for structural damage mechanisms such as fastener corrosion and wood decay. Here, we present the first measurements of electrical resistance of southern pine at the subcellular level as a function of wood MC by using a 1-μm-diameter probe. In latewood, measurements were taken in both the secondary cell wall (S2) and the cell corner compound middle lamella (CCCML). In earlywood, measurements were only possible in the CCCML. As expected,

* Corresponding author
† SWST member
[1] This article was written and prepared by US Government employees on official time, and it is therefore in the public domain and not subject to copyright.

Wood and Fiber Science, 48(2015 Convention, Special Issue), 2016, pp. 54-61

resistance decreased with increasing relative humidity (RH) in all locations. Resistance decreased more rapidly with RH in the S2 layer than in any of the middle lamellae. These results give insight into how some moisture-dependent wood properties affecting ion movement may be partitioned across cell wall layers.

Keywords: Wood–moisture relations, wood electrical properties, timber physics, percolation theory, wood damage mechanisms.

INTRODUCTION

Wood–moisture relations have long been studied using electrical measurements at the macroscopic level (Stamm 1929; Hearle 1953; James 1963; Zelinka et al 2007, 2008b). The electrical conductivity of wood, σ and its reciprocal, the resistivity, ρ are material properties that depend strongly on wood MC. These material properties are directly related to the resistance of wood, R, which can easily be measured, but R depends on the electrode geometry, whereas σ and ρ do not (Hummel 2001). For special boundary conditions, σ and ρ can be calculated from R. For example, under a uniform electric field, R is proportional to the distance between the electrodes and inversely proportional to the cross-sectional area of the conductor.

Recently, Zelinka et al (2008a) proposed a new mechanism for electrical conduction in wood based on percolation theory. The theory describes the rapid increase in conductivity of wood as a function of MC between roughly 15% and 30% MC in terms of a percolating network through which ion movement occurs. One key feature of the model is that there is a percolation threshold, which is the MC at which the percolating network first forms and below which ionic conduction cannot occur. Above the percolation threshold, conductivity increases with a power-law behavior. Because the percolation threshold represents the lower bound for ionic conduction, it also represents the MC below which wood damage mechanisms that rely on ion transport, such as fastener corrosion (Baker 1980, 1988) and wood decay (Griffin 1977; Viitanen and Paajanen 1988; Carll and Highley 1999; Wang and Morris 2010), cannot occur (Jakes et al 2013).

Jakes et al (2013) developed a model for chemical movement in cell walls that is consistent with the percolation model for ionic conduction. In this model, chemical movement occurs in regions of the cell in which the hemicelluloses have gone through a moisture-induced glass transition. In dry conditions, hemicelluloses in wood have a glass transition between 150°C and 220°C. However, the glass transition temperature decreases with MC and eventually crosses room temperature when in equilibrium with a relative humidity (RH) of approximately 60-80% (Cousins 1976, 1978; Kelley et al 1987; Olsson and Salmén 2004). Above the glass transition temperature, hemicellulose backbones twist and bend facilitating the movement of ions and other chemicals between energetically favorable sites. Just below the percolation threshold, some hemicelluloses have adsorbed enough moisture to soften at room temperature. As RH increases, the number and size of softened regions grow until they form a continuous pathway through which chemicals and ions can exhibit long-range diffusion.

The percolation model developed by Zelinka et al (2008a) was based on macroscale measurements of electrical conductivity and implicitly treats the wood material as homogenous. The transport mechanism proposed by Jakes et al (2013) depends on a moisture-induced glass transition occurring in the hemicelluloses. This theory suggests that there are probably differences in the threshold MC for chemical transport among the different regions in the cell wall as a function of the differing relative abundance and orientation of hemicelluloses. For instance, the secondary cell wall (S2) contains cellulose microfibrils, amorphous cellulose, hemicelluloses, and lignin and the hemicelluloses are preferentially oriented along the microfibrils (Åkerholm and Salmén 2001; Stevanic and Salmén 2009). In contrast, in the compound middle lamella, hemicelluloses exist in an irregular network of lignin (Hafren et al 2000). Because there are differences

in the orientation and amount of hemicelluloses between the S2 and the compound middle lamella, we hypothesized that these cell wall domains might exhibit differences in how conductivity increases with moisture and that such differences may give further insight into moisture-induced changes in wood.

MATERIALS AND METHODS

Tests were conducted on microtome-cut transverse sections of southern pine (*Pinus* spp.) wood. Although the exact species was not determined when felled, the tree was harvested from a plantation in which more than 90% of the trees were slash pine (*Pinus elliottii*). Section thickness was examined as an experimental variable and was controlled with the microtome thickness settings: measurements were taken on 20-, 40-, and 60-µm sections. Sections were stored in 50% ethanol to prevent microbial degradation. Immediately prior to testing, the sections were rinsed with water, placed in the sample holder, and conditioned at 50% RH and 22°C. In addition, measurements were attempted on 500-µm sections cut by a fine saw. However, the surface roughness of these samples precluded reproducible results.

Making electrical contact with the wood sample was challenging. To ensure good electrical contact, a sample holder was developed to press the section on a conductive metal plate while allowing the top to be accessed and to exchange moisture with the environment. The sample holder consisted of an acrylic plate with a hole in the center (Fig 1). The section sat between the acrylic plate and an aluminum plate, which was used as one of the electrodes. Bolts were used to tighten the acrylic plate to the aluminum plate, and an extra bolt was attached to the aluminum, allowing a wire to be connected to it for the electrical measurements. The second electrode in the measurement was a tungsten probe with a 1-µm tip diameter (Electron Microscopy Sciences, Hartfield, PA). This measurement technique is influenced by deformation of the tip, contact between the tip and the specimen, contact of the specimen with the bottom of the sample holder, and how contact might be affected by swelling of the specimen as RH increases. Although, care was taken to take the measurements the same way every time, we do not have a quantitative estimate of how these contact variables affected resistance measurements.

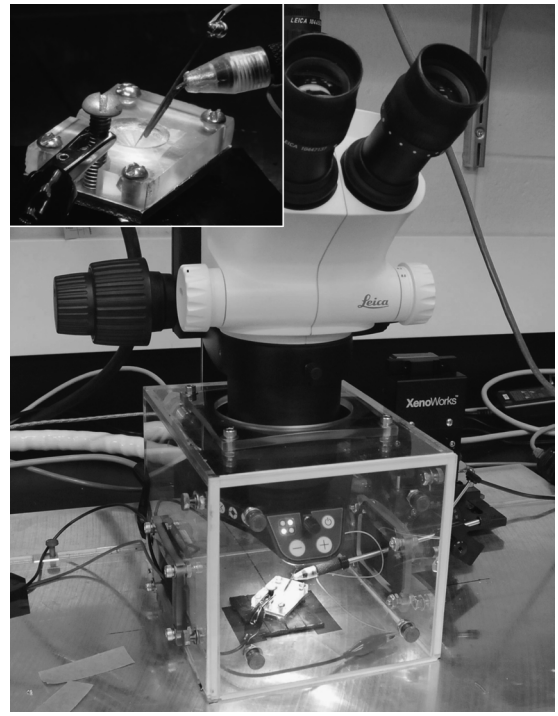

Figure 1. Experimental setup showing the micromanipulator inside the RH chamber built around a stereoscope. Inset: close-up view of the sample holder.

Measurements were taken in a custom chamber built around an S8APO stereomicroscope (Leica, Wetzlar, Germany) (Fig 1). The chamber was built to house the tungsten probe and the objective of the stereomicroscope. The probe was positioned with a Xenoworks micromanipulator (Sutter, Novato, CA) with a minimum step size of 62.5 nm. Constant RH was maintained by a 2 L/min flow of conditioned air into the chamber from a HumiSys RH generator (InstruQuest, Coconut Creek, FL) that relied on a RH sensor placed inside the chamber.

For each RH condition, the probe was placed in contact with 10 replicates of a given cell wall

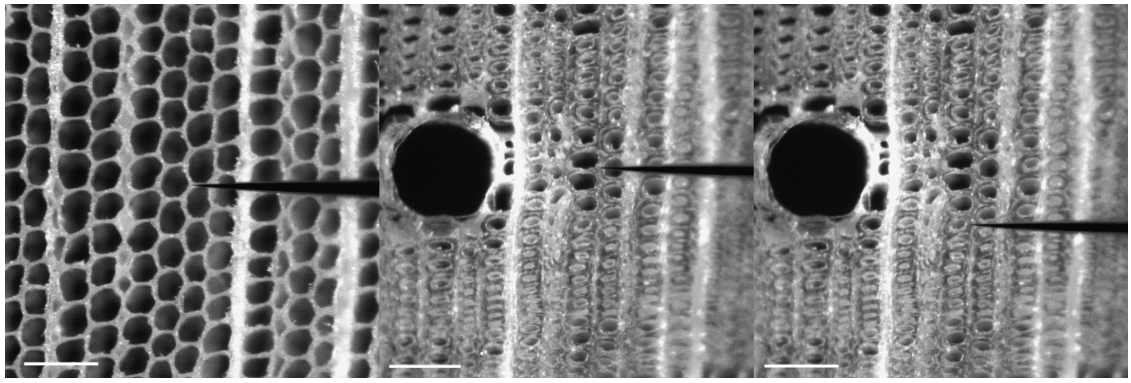

Figure 2. Probe tip in the CCCML (earlywood), CCCML (latewood), and the S2 (latewood) (left to right). Scale bar represents 100 μm.

domain, and the electrical resistance was measured. RH was then increased, and the section was allowed to condition for 25 min at the new RH. Then the measurements were repeated on the same 10 cell wall domains that had been measured at the previous RH condition. Measurements were taken at seven different RH conditions starting at 50% (50%, 57%, 64%, 71%, 78%, 85%, and 95%).

Within the latewood, measurements were taken in the cell corner compound middle lamella (CCCML) and the S2 (Fig 2). Because the cell walls of earlywood tracheids are only approximately twice as thick as our probe tip, the S2 cell wall layer could not be individually measured and only the CCCML was measured. This allowed us to compare the electrical conductivity of one cell wall domain (CCCML) across two growth ring domains, to determine if growth ring domain influenced electrical conductivity at this scale.

The resistance measurements were performed with an apparatus designed to minimize polarization effects and to allow for consistent and repeatable measurements (Boardman et al 2012). The system applied 10 V across a 10-MΩ precision resistor in series with the specimen; polarization was prevented by switching the polarity of the bias voltage at a frequency of 1 Hz and averaging four measurements. The resistance of the wood was determined from measuring the voltage drop across the precision resistor, resulting in uncertainty of less than 20% at 50 GΩ.

Statistical comparisons among measurements taken at different section thicknesses, cell wall domains, and growth ring domains were made using *t*-tests. Two different types of comparisons were made. Paired *t*-tests were used to compare the mean values at each RH. This resulted in a single p value for a comparison between the two resistances vs RH curves. In addition, unpaired *t*-tests assuming unequal variances (heteroscedastic) were calculated from the 10 replicates at each RH condition. This resulted in a p value at each RH.

RESULTS AND DISCUSSION

Figure 3 contains mean resistance as a function of RH for all of the different sample groups. A statistical comparison of the data sets is given in Tables 1 and 2. From these data, three major trends can be observed: the resistance of the S2 layer exhibited a different dependence on RH than the CCCML, CCCML measurements were independent of growth ring domain, and the resistance in the CCCML depended on both sample thickness and RH.

Clear differences can be observed between the curves representing the S2 layer and the CCCML, and it is not surprising that they are statistically significantly different ($p = 0.003$, Table 2). At greater than 50% RH, the S2 layer

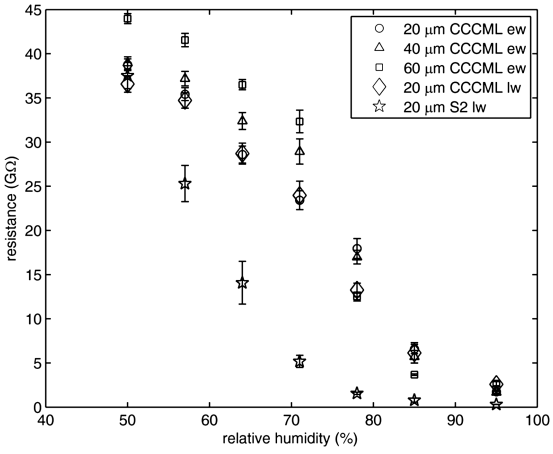

Figure 3. Mean resistance at each RH condition. Error bars represent the standard error (CCCML; ew, earlywood; lw, latewood; S2).

had a lower resistance than the CCCML and exhibited a sharp decrease between 57% and 71% RH. In contrast, the CCCML had an almost linear decrease in resistance between 50% and 71% RH, whereas a sharp decrease in resistance was observed between 71% and 78% RH.

For 20-μm-thick sections, measurements were taken in the CCCML of both the earlywood and latewood domain. Visually, these data (represented by the C and ◊, respectively) are difficult to separate on the plot. Using a paired *t*-test for the mean values at each RH, the data for earlywood and latewood CCCML were not statistically different ($p = 0.25$). These data indicate that the electrical properties of the CCCML do not depend on the growth ring domain. Furthermore, large measured differences between the S2 layer and the CCCML support our tacit assumption that our measurements of the S2 were largely unaffected by the near proximity of the CCCML.

Measurements taken in the earlywood CCCML at different section thicknesses are shown in Fig 4. Resistance is plotted as a function of section thickness, with the different RH conditions shown as different symbols. For RH conditions from 50% to 71% as well as 95%, resistance increased with increasing sample thickness. At 78% and 85% RH, however, resistance decreased with increasing sample thickness. Table 1 indicates that *p* values were largely nonsignificant when comparing 20- to 40-μm sections and predominantly highly significant from 40- to 60-μm sections and 20- to 60-μm sections. Further work is needed to

Table 1. The *p* values from unpaired heteroscedastic *t*-tests of 10 measurements at each RH condition.[a]

Growth ring domain	EW			EW to LW	LW
Cell wall domain	CCCML			CCCML	CCCML to S2
Section thickness (μm)	20-40	40-60	20-60	20	20
50% RH	0.833	$p << 0.001$	$p << 0.001$	0.021	0.542
57% RH	0.111	0.001	$p << 0.001$	0.434	0.005
64% RH	0.008	0.002	$p << 0.001$	0.929	0.001
71% RH	0.005	0.079	$p << 0.001$	0.707	$p << 0.001$
78% RH	0.463	$p << 0.001$	0.001	0.002	$p << 0.001$
85% RH	0.309	0.014	$p << 0.001$	0.626	$p << 0.001$
95% RH	0.797	0.007	0.005	0.004	$p << 0.001$

[a] EW, earlywood; LW, latewood.

Table 2. The *t*-tests of paired mean values at each RH condition.[a]

Growth ring domain	Cell wall domain	Section thickness	*p* value
EW	CCCML	20-40	0.206
EW	CCCML	40-60	0.280
EW	CCCML	20-60	0.207
EW-LW	CCCML	20	0.250
LW	CCCML to S2	20	0.003

[a] EW, earlywood; LW, latewood.

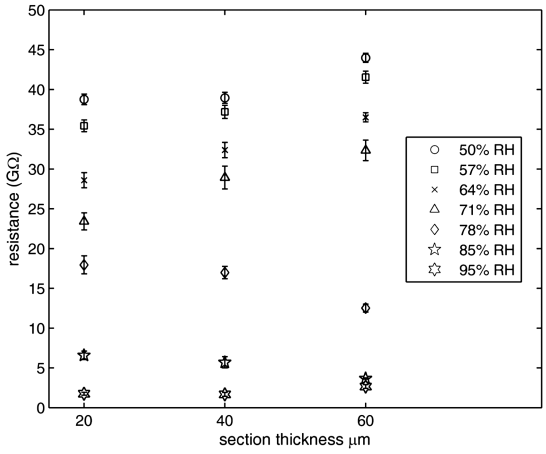

Figure 4. Mean resistance as a function of section thickness for measurements taken in the CCCML (earlywood). Error bars represent the standard error.

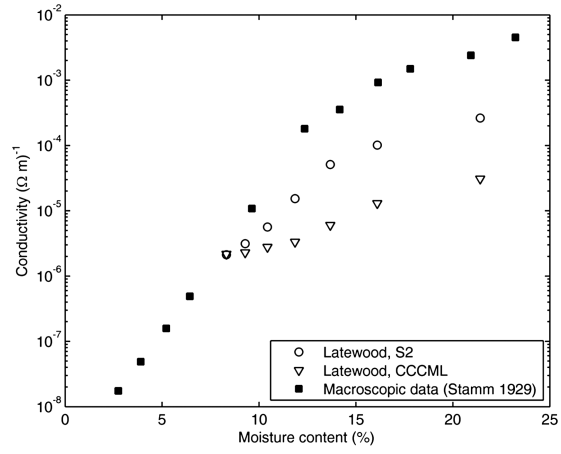

Figure 5. Latewood measurements from the S2 and CCCML converted to conductivity values and compared with historical, macroscopic data.

understand why resistance decreases with section thickness at 78% and 85% RH.

It is worthwhile to compare these data to those collected at the macroscale. Traditionally, electrical measurements in wood have been plotted as conductivity (σ, the reciprocal of the resistivity, ρ) as a function of the wood MC. To convert the data in Fig 3 to conductivity values, we used the analytical solution to the Laplace equation for a point-source electrical field:

$$\frac{1}{\sigma} = \rho = 4\pi r R \qquad (1)$$

where r is the radius of curvature of the electrode and R is the measured resistance (Telford et al 1990). The relationship between the RH and MC comes from macroscopic water vapor sorption isotherm measurements on the same parent board (Zelinka et al 2014). This transformation, therefore, assumes that the sorption isotherms of the CCCML and the S2 layer are the same. Although there are probably differences between the CCCML and the S2 isotherms, there are no data on these layers individually although Browning has studied differences in liquid water absorption between these layers (Browning 1963). The macroscopic data incorporate signals from both the S2 and the CCCML in both earlywood and latewood, with no ability to separate either cell wall or growth ring domains. We plotted these transformed data in Fig 5 on the same axis as the macroscopic data used to construct the percolation model (Stamm 1929; Zelinka et al 2008a).

In Fig 5, measurements from the S2 layer closely follow the shape of the macroscopic data curve, except that they are lower in magnitude than the macroscopic data by less than one order of magnitude (the data are presented on a logarithmic scale). This strongly suggests that our data represent resistance measurements of the various wood domains as opposed to solely an interfacial resistance or an experimental artifact. Furthermore, Zelinka et al (2008a) noted that the shape of Stamm's conductivity as a function of MC data were consistent with a percolating system. This similar curvature in the S2 layer suggests the formation of a percolating network in the S2 layer as well and that bulk wood electrical properties are dominated by the S2.

In mesoscale measurements of the wood cell wall with a probe diameter of 0.5 mm and a path length of 10-50 mm, Zelinka et al (2015b) observed that resistance of earlywood was greater than that of latewood in southern pine conditioned at 95% RH. They attributed differences between earlywood and latewood to a greater specific

gravity in the latewood, because the lumen is nonconducting. These subcellular scale measurements show that differences in electrical conductivity between earlywood and latewood also may be influenced by differences in the conductivity and relative proportions of middle lamella and S2 in each growth ring domain, rather than specific gravity of the bulk tissue alone.

Measurements taken in the S2 and the CCCML exhibited sharp decreases in resistance in the ranges of 57-71% RH and 71-78% RH, respectively (Fig 3). One possibility is that these decreases corresponded with the threshold for ion movement in wood cell walls. Zelinka et al (2015a) used synchrotron-based X-ray fluorescence microscopy to examine the movement of implanted ions through the wood cell wall as a function of RH. Depending on the ions (K^+, Cl^-, Cu^{2+}, or Zn^{2+}), they observed that the threshold for ion movement varied between 60% and 90% RH, which is the same RH regime for which slope changes in the S2 and the CCCML were evident.

If chemical movement is indeed a necessary criterion for wood damage mechanisms, as proposed by Jakes et al (2013), these measurements suggest that there are differences between the two cell wall layers examined in their moisture-dependent transport mechanisms. Specifically, in the S2 layer in which the hemicelluloses are more regularly oriented, there is a sharp increase in conductivity between 57% and 71% RH and the conductivity data are similar to the macroscopic data, which has been fit with a percolation model. In contrast, in the middle lamella, there appears to be a sharp increase in conductivity with MC between 71% and 78% RH, but the curve does not appear to fit the same percolation model as the S2 data under the assumption that different cell wall domains have the same sorption isotherm. If a rapid increase in conductivity is indeed controlled by the hemicelluloses passing through a moisture-induced glass transition, then these measurements suggest that the nature of this moisture-induced softening is different in the S2 layer and the middle lamella. Further work examining chemically modified cell walls may give further insight into the transport mechanism and how these chemical modifications impart decay resistance to the wood.

Although our method shows promise as a way to potentially investigate chemically modified wood, the limitations of this approach should also be discussed. The major limitation is ensuring good contact between the tip, the wood cell wall, and the conducting plate. The measurements required refinement in pressing the wood cell tightly to the conducting plate while allowing the probe tip to touch the top of the sample. Furthermore, the probe tips were extremely easy to plastically deform when touching the cell wall, even when controlled by the micromanipulator. Together, these experimental difficulties required a highly skilled operator to place the probe tip, and it is unclear what sort of systematic errors might have been caused by how the probe was placed. Despite these difficulties and potential systematic errors, the fact that there appeared to be differences between the S2 layer and the middle lamella, gave some credence to the measurements.

CONCLUSIONS

Electrical resistance was measured through microtomed wood sections as a function of RH using a 1-μm-diameter tungsten probe contacting the S2 and the CCCML of southern pine. Several conclusions can be drawn from these measurements:

1. Resistance of the CCCML was measured in both earlywood and latewood. On average, there was no significant difference between resistance of the CCCML measurements in earlywood and latewood. In latewood, in which measurements were taken in both the S2 and the CCCML, moisture dependence of the two cell wall layers was different. Together, these data show that electrical resistance of wood cell walls depends on moisture and cell wall domain but not growth ring position.
2. When plotted against historic, macroscopic data of conductivity as a function of MC, conductivity of S2 closely mimicked the macroscopic conductivity, in contrast to measurements in the CCCML, which behaved differently.

3. Measurements from both cell wall domains suggest that in both cell wall layers, there is percolation-type behavior.
4. Future work using this technique could probe electrical conductance mechanisms in different cell wall layers and examine the effect of chemical modifications on conductance within different cell wall layers.

REFERENCES

Åkerholm M, Salmén L (2001) Interactions between wood polymers studied by dynamic FT-IR spectroscopy. Polymer (Guildf) 42(3):963-969.

Baker AJ (1980) Corrosion of metal in wood products. Pages 981-993 *in* Durability of building materials and components. ASTM STP 691. American Society for Testing and Materials, West Conshohocken, PA.

Baker AJ (1988) Corrosion of metals in preservative-treated wood. Pages 99-101 *in* Wood protection techniques and the use of treated wood in construction. Forest Products Society, Madison, WI.

Boardman C, Glass SV, Carll CG (2012) Moisture meter calibrations for untreated and ACQ-treated southern yellow pine lumber and plywood. J Test Eval 40(1):1.

Browning BL (1963) The chemistry of wood. Interscience Publishers, New York. 689 pp.

Carll C, Highley TL (1999) Decay of wood and wood-based products above ground in buildings. J Test Eval 27(2): 150-158.

Cousins W (1976) Elastic modulus of lignin as related to moisture content. Wood Sci Technol 10(1):9-17.

Cousins W (1978) Young's modulus of hemicellulose as related to moisture content. Wood Sci Technol 12(3): 161-167.

Griffin D (1977) Water potential and wood-decay fungi. Ann Rev Phytopathol 15(1):319-329.

Hafren J, Fujino T, Itoh T, Westermark U, Terashima N (2000) Ultrastructural changes in the compound middle lamella of *Pinus thunbergii* during lignification and lignin removal. Holzforschung 54(3):234-240.

Hearle JWS (1953) The electrical resistance of textile materials: IV. Theory. J Text I 44:T177-T198.

Hummel RE (2001) Electronic properties of materials. 3rd ed. Springer, New York, NY.

Jakes JE, Plaza N, Stone DS, Hunt CG, Glass SV, Zelinka SL (2013) Mechanism of transport through wood cell wall polymers. J Forest Prod and Ind 2(6):10-13.

James WL (1963) Electric moisture meters for wood. Res Note FPL-08. USDA For Serv Forest Prod Lab, Madison, WI.

Kelley SS, Rials TG, Glasser WG (1987) Relaxation behaviour of the amorphous components of wood. J Mater Sci 22(2):617-624.

Olsson A-m, Salmén L (2004) The softening behavior of hemicelluloses related to moisture. Pages 184-197 *in* ACS symposium series 1999. American Chemical Society, Washington, DC.

Stamm AJ (1929) The fiber-saturation point of wood as obtained from electrical conductivity measurements. Ind Eng Chem Anal Ed 1(2):94-97.

Stevanic JS, Salmén L (2009) Orientation of the wood polymers in the cell wall of spruce wood fibres. Holzforschung 63(5):497-503.

Telford WM, Geldard LP, Sheriff RE (1990) Chapter 8. Resistivity methods. Pages 522-577 *in* Applied geophysics. Cambridge University Press, Cambridge.

Viitanen H, Paajanen L (1988) The critical moisture and temperature conditions for the growth of some mould fungi and the brown rot fungus Coniophora puteana on wood. Paper read at International Research Group on Wood Protection, Madrid, Spain.

Wang J, Morris PI (2010) A review on conditions for decay initiation and progression. Paper number IRG/WP 10-20444 *in* International Research Group on Wood Protection. IRG Secretariat, Biarritz, France.

Zelinka S, Glass S, Stone D (2008a) A percolation model for electrical conduction in wood with implications for wood-water relations. Wood Fiber Sci 40(4):544-552.

Zelinka SL, Gleber S-C, Vogt S, Rodríguez López Gabriela M, Jakes Joseph E (2015a) Threshold for ion movements in wood cell walls below fiber saturation observed by X-ray fluorescence microscopy (XFM). Holzforschung 69(4):441-448.

Zelinka SL, Glass SV, Boardman CR, Derome D (2014) Moisture storage and transport properties of preservative treated and untreated southern pine wood. Wood Mater Sci Eng:1-11. doi:10.1080/17480272.2014.973443.

Zelinka SL, Rammer DR, Stone DS (2008b) Impedance spectroscopy and circuit modeling of Southern pine above 20% moisture content. Holzforschung 62(6):737-744.

Zelinka SL, Stone DS, Rammer DR (2007) Equivalent circuit modeling of wood at 12% moisture content. Wood Fiber Sci 39(4):556-565.

Zelinka SL, Wiedenhoeft AC, Glass SV, Ruffinatto F (2015b) Anatomically informed mesoscale electrical impedance spectroscopy in southern pine and the electric field distribution for pin-type electric moisture metres. Wood Mater Sci Eng 10(2):189-196.